STM JOURNALS

Journal of
Polymer & Composites

ISSN: 2321-2810 (Online)
ISSN: 2321-8525 (Print)
Volume 14, Issue 4, 2026
DOI (Journal): 10.37591/JoPC

https://journals.stmjournals.com/jopc

Research JoPC

Enhanced Mechanical Properties of AZ31 Magnesium Alloy Composite Reinforced with Carbon Nanotubes and Nano hydroxyapatite

Ashu Tyagi[1,*], Pardeep Kumar[2]

Abstract

Magnesium alloys represent a novel category of biodegradable materials, offering numerous advantages in addressing the limitations associated with conventional biomedical materials. Magnesium-based metallic biomaterials offer a promising solution for fixing fractures, ensuring effective treatment without the inconvenience of subsequent implant removal procedures. In the present work, AZ31 Mg-alloy was chosen as the base material. Five specimens were meticulously fabricated, each varying in weight percentages of reinforcement materials: 0wt%, 0.5wt%, 1wt%, 2wt%, and 4wt% of carbon nanotubes (CNTs), while the weight of nanohydroxyapatite (nHA) remained constant at 0.5 wt%. Friction stir casting was the chosen fabrication method for the specimens. The EDS results reveals that the components such as C, Zn, Ca, P, O, Mg, and Al are present in desired proportions on the sample surface. Addition of CNTs/nHA significantly enhanced the tensile strength, compressive strength, and micro-hardness of the AZ31 matrix, and values are 25.65%, 153.3%, and 41.26% higher than pure AZ31 matrix, respectively. The porosity of the composites has increased with the increase in the content of CNTs, and its values were 0.43%, 2.18%, 2.34%, 2.48 %, and 5.3% at 0 wt% 0.5 wt%, 1 wt%, 2 wt%, and 4 wt% respectively. The newly developed AZ31 alloy composite is stronger and may be utilised in bone implants and biomedical applications.

Keyword: Magnesium alloy; carbon nanotube; hydroxyapatite; mechanical characteristics; microstructure; friction stir casting

INTRODUCTION

Metallic biomaterials are favored for temporary tissue applications owing to their ability to bear loads. Among these materials, magnesium-based ones stand out due to their unique combination of desirable biological properties [1–3]. They degrade naturally within the physiological environment while still providing robust load-bearing support. Thus, magnesium-based metallic biomaterials offer a promising solution for fixing fractures, ensuring effective treatment without the inconvenience of subsequent implant removal procedures [4–6]. Magnesium and the natural bone has similar mechanical characteristics, which reduces the stress-induced observed with other materials. However, magnesium deteriorates swiftly in the biological surroundings, producing magnesium hydroxide via the evolution of hydrogen during the deterioration phase [7–9]. As the decomposition rate is slow, the resulting H_2 gas is utilized by the developing cells and high deterioration rate may create a sub-facial pocket generated by the gas at the connection of implant and tissues. It is noted that the hydrogen gas produced during breakdown

***Author for Correspondence**
Ashu Tyagi
E-mail: tyagiashu236@gmail.com

[1]Research Scholar, Department of mechanical engineering, Deenbandhu Chhotu Ram University of Science and Technology, Murthal, Sonipat, Haryana, India
[2]Assistant Professor, Department of mechanical engineering, Deenbandhu Chhotu Ram University of Science and Technology, Murthal, Sonipat, Haryana, India

Received Date: August 01, 2025
Accepted Date: August 19, 2025
Published Date: June 27, 2026

Citation: Ashu Tyagi, Pardeep Kumar. Enhanced Mechanical Properties of AZ31 Magnesium Alloy Composite Reinforced with Carbon Nanotubes and Nano hydroxyapatite. Journal of Polymer & Composites. 2026; 14(4): 206–217p.

of magnesium implants vanishes entirely within 6 weeks and seldom causes difficulties. However, fast deterioration has an impact on contacts of materials and tissues that rely on cell activity. So, preventing quick degradation is crucial in the development of magnesium-based bio-absorbable prostheses [10–14].

The deterioration rate of magnesium may be reduced through the development of novel materials made of composites applying surface coatings, and changing its micro-structure [15–17]. Hydroxyapatite (HA) has drawn significant interest during the last 20 years because of its superior biological compatibility, bio mineralization, and good strength. There are limited work done on fabrication of Mg/HA nanocomposite by powder sintering methods. In addition, much work has been done to increase the durability of several Mg-alloys by coating their surfaces with HA. However, since deterioration begins at the magnesium's surface, adding HA into the surface may provide superior protection by making the matrix surface better bioactive [18–20]. In the past researches, the Friction Stir Processing successfully developed AZ91D-SiO2 surface coatings for potential use in biomedical prostheses [21–24]. Yousefpour et al. (2022b) developed a nanocomposite of Mg-alloy, nHA, and mAg to study its tensile behaviour for biomedical applications [25]. Vidal et al. (2022) [26] investigated how adding HA and FA nanofillers to the Mg-alloy matrix affected biodegradation and cytotoxicity. Mg-HA nanocomposite was discovered to be the superior biocomposite material for bone implants due to its biocompatible behaviour and strength similar to bone in previous studies [27–30]. Mg-alloys such as AZ91, AZ31, and others were discovered to be suitable materials for implantation due to their closer strength as that of bone resulting in reduced stress induced within the bone and implants interactions. These desired properties make Mg-alloy composites a viable option for implants [31]. AZ31 is strengthened by biologically compatible, bioresorbable, and biomaterial-grade reinforcements such as carbon nanotube, Graphene, HA, and Titanium oxide. The biological compatibility of a material refers to its capacity to fulfill the needed functionality while enabling host reactions to take place in the human organism. On the basis of present demand, biocompatible implants are quickly rising to treat bone injuries, degradation from mishaps, sports injuries, and so on. The material used in the implants is often referred to as a smart prosthesis [32–35]. CNT has outstanding features such as a high yield strength of 150GPa approx. and an elastic modulus of around 1TPa, as well as being compact, high performing, and having a high aspect ratio, which make it useful as a reinforcing agent [36]. CNT's biocompatibility makes it ideal for usage in implants for biomedical purposes. In the current investigation, a multi-walled CNT is utilised as a strengthening substance [37]. The bone has a complicated geometry made up of nano-hydroxyapatite (nHA), collagen, and non-collagenous components [38]. The biological system accounts for about 25% of calcification bones, in addition to 2–5% tissue cells, 5% water-based, and 70% inorganic nHA. Tissue engineers are drawn to generating bone tissue and employing entirely produced and naturally obtained nano hydroxyapatite because it is so comparable to how bone is generally created [39, 40].

This research article delves in producing an Mg-based hybrid nanocomposites reinforced by both carbon nanotubes (CNT) and nano-hydroxyapatite (nHA) through friction stir casting. The main aim of this work is to meticulously examine the microstructure as well as the mechanical characteristics of the novel composite matrix across different compositions.

MATERIALS AND METHODS

Composite Preparation

In the present work, AZ31 magnesium alloy was selected as the base material, possessing the composition (wt %) of Al-5.86, Zn-0.73, Mn-0.25, Cu-0.0009, Fe-0.006, and remaining Mg. Five specimens were meticulously fabricated, each varying in weight percentages of reinforcement materials: 1wt%, 2wt%, and 4wt% of carbon nanotubes (CNTs), while the weight of nanohydroxyapatite (nHA) remained constant at 0.5 wt%. Both CNTs and nHA, in powder form, were selected based on their unique mechanical and bioactive properties, intended to impart synergistic enhancements to the AZ31 matrix. Friction stir casting was the chosen fabrication method for the specimens as shown in Figure 1, ensuring efficient mixing and distribution of the reinforcement materials. The process parameter of friction stir casting are shown in Table 1. The fabrication process

commenced with the magnesium sheet placed in a stir casting furnace under an argon atmosphere to prevent oxidation, followed by heating to 800°C until reaching a molten state. Subsequently, the furnace temperature was lowered to 500°C, maintaining a semi-liquid state, and preheated CNTs and nHA powders were added to the molten AZ31. The temperature of furnace was risen to 850°C, and the liquidized composite was stirred for 10 minutes at 450 rpm to achieve homogeneous blending with the base material. The composite blend was then poured into a cylindrical die and allowed to cool, with the entire fabrication process spanning 7 hours per specimen, including 4 hours in the friction stir casting furnace and an additional 3 hours for cooling. This meticulous procedure was iterated for all five composite specimens, ensuring consistency and reproducibility in the fabrication process for subsequent analysis and characterization.

Physical and Mechanical Properties

The porosity is the measure of the pores present within the material. Four square shaped samples of each composite were taken to measure the porosity. The Archimedes principal was used to measure the actual density of the specimens. The specimens were weighed in both air and distilled water with the help of weighing machine with accuracy of 0.01mg. The theoretical density was calculated by ratio of mass to volume of the composite specimens. However, the porosity will be calculated as follows:

$$\text{Porosity } (\%) = [1 - (\rho_a / \rho_t)] \times 100$$

$$\rho_a = [W_a / (W_a - W_w)] \times \rho_w$$

Where,
W_w: specimen's weight in distilled water
W_a: specimen's weight in still air
ρ_a: actual density of samples
ρ_w: water density
ρ_t: calculated density of specimens

Table 1. Casting process parameter.

Parameter	Value
Stirring temperature (Max.)	850°C
Preheating temperature for reinforcement	450–500°C
Stirring velocity	240–300 rpm
Stirring time in furnace	10 mins
Preheat temperature for die	260°C
Casting time	4 hours
Cooling time in die	3 hours

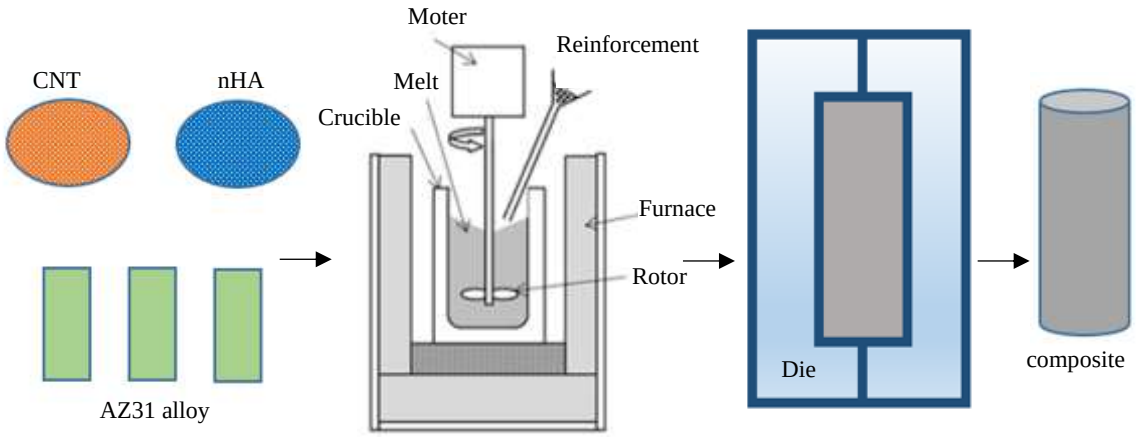

Figure 1. Method of composite preparation.

Three tensile samples of five millimeters in diameter and twenty-five millimeters gauge length were produced from every material using wire-cut EDM parallel to the extrusion direction. The tensile tests were done by using a FIE UNITEK 94100 UTM with speed of 5mm/min as per ASTM standards. Compression tests were conducted on samples (20 mm × 20 mm × 20 mm) using the same UTM with compressive fixtures at speed of 2 mm per minute. The mean values of these specimens was calculated to measure the results of both the tensile and compression strength. The micro-Vickers hardness tester is a common instrument to measure the hardness of the composites. The composite material specimens were prepared by cutting rectangular blocks with an EDM, polishing them, and then cleaning to achieve a smooth and level surface for testing. Micro hardness was evaluated using Micro-Vickers hardness testing equipment fitted with a pyramid-shaped diamond indenter with a square base under a 300 N load and a dwell duration of 10 seconds. The mean values of four indents for every specimen was used in the findings.

CHARACTERIZATION

The composite materials were analyzed by using the EDS to find out their elemental composition. X-rays were shot on the sample, which causes each atom in the sample to emit its characteristic X-rays. The X-rays, after they are detected and analyzed, can then specify the elemental content of the sample. This particular analysis will likely be carried out by defining whether and where CNT, nHA and AZ31 alloy (consisting mainly of Mg, Al and Zn) are present. Through the proportions of the heights of the peaks represents the characteristic X-rays emitted by each element, the quantities of the components can be quantified to have an idea about the material's composition.

Scanning electron microscopy is used to examine materials' anatomical properties. During this method, electrons are released from the entire surface of the specimen. The morphological characteristics, link development, cracks, and aggregation were all investigated using an SEM. Samples measuring 25 × 15 × 6 mm have been extracted from the composite specimen for analysis of microstructural characteristics. They were then manually polished with abrasive paper rated up to 2500 grades and washed with ethanol. Furthermore, the specimens were polished using gemstone paste using a buffing device. The specimens were ultrasonically washed in ethanol to eliminate any polishing residues. The refined specimens were then wiped using a solution having 10 mL of CH3COOH, 20 mL of H2O, and 100 mL of C2H5OH for one minute. Then microstructural studies were performed using a SEM operating at 10 kV.

RESULT AND DISCUSSION

EDS and SEM Analysis of the CNT & nHA Reinforced AZ31 Mg Alloys

Figure 2 shows the EDS findings from the specimen's surfaces. When an EDS examination of the strengthened samples is performed, it is discovered that the primary ingredients employed in the manufacturing of CNT/nHA composites are present in the matrix. As shown in Figure 2, the specimen's surface contains components such as C, Zn, Ca, P, O, Mg, and Al. There are low-level oxygen spikes. The EDS analysis reveals that composites provide excellent protection against oxygen from the surrounding's absorption throughout the production process. This is due to the mixing was done via a tiny hole built on the top of the furnace, while the melting process was carried out in an enclosed chamber. To prevent Mg oxidation, the gas shielding of argon gas was done to provide an inert atmosphere, as indicated in the picture. Carbon (C), phosphorus (P), and calcium (Ca) particles present in composite materials are apparent in the spectrum. It has been observed that when reinforcement increases, so do the content peaks of C, P, and Ca, resulting in a well dispersion of reinforced elements in the magnesium alloy. As a consequence, the acquired EDS analysis findings suggest that friction stir casting is an effective approach for creating reinforced composites with the appropriate component proportions.

SEM is used to analyse the morphological characteristics of materials. During this procedure, electrons are emitted over the whole surface of the sample. All photos depict particle distributions of

all metallic and non-metallic components, with particles dispersed uniformly in the magnesium matrix. However, certain agglomerations have been identified in the morphology of the AZ31 nanocomposite. According to Huang et al. (2016a) and Sivanesh Prabhu et al. (2020), multi-pass FSP may enhance the dispersion of reinforcing particles in a metal matrix. The consistent distribution of nanoparticles is the result of repetitive mechanical churning at extreme temperatures.

Figure 3 depicts the overwhelming majority of carbon nanotubes noticed at magnesium grain boundaries. They also appeared dispersed in an individual fiber form, as seen in Figure 3 from a SEM inspection of the scraped substrate using 0.04 percent HCl solutions for 40 seconds. As a consequence, when enough quantities of CNTs are injected, the strengthened surface of the Mg domains becomes highly susceptible to deformity, resulting to enhanced tensile properties. The nHA particles had an acicular shape, measuring 15–20 nm wide and 60–80 nm long. The nHA nanoparticles and CNTs reduced the size of the granules in the matrix, making it more homogeneous. The results obtained are comparable to those of prior investigations [41–43]. The nHA particles are located at the middle of many dimples. This suggests that interaction of particles and matrix have the ability to form microvoids. The nanocomposites' tiny bumps may be attributed to their reduced grain size (a larger proportion of grain borders) and the inclusion of nHA particles. Fractures may happen at corners of grains, crossings, and interactions, with very tiny voids forming and then sliding and/or rotating to generate intergranular microcracks [44]. The microvoids and microcracks proliferate and merge to generate larger voids and fractures. Because the matrix is not very ductile, tiny voids and cracks in the Mg-based composite connect quickly.

Mechanical Behavior of AZ31/CNT/nHA Composite

The characteristics of newly developed composite was obtained by various methods as explained in section 2. The mechanical and physical characteristics of AZ31 alloy and AZ31/CNT/nHA composites are enlisted in Table 2.

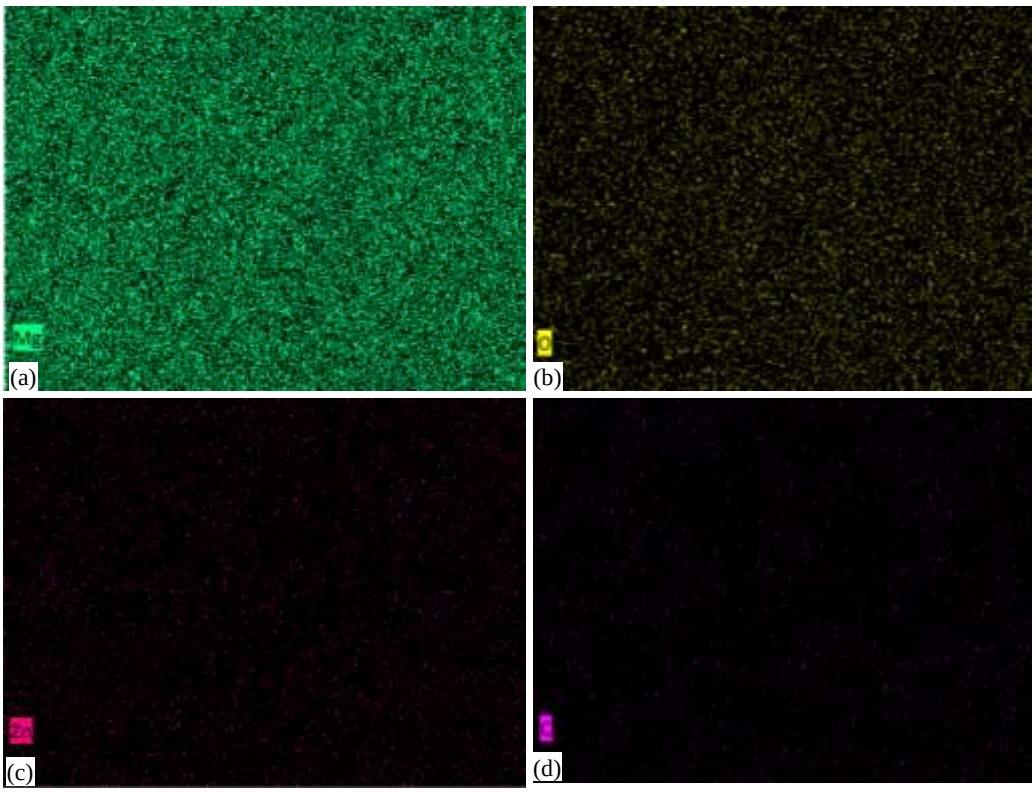

Figure 2. EDS results are depicting the elemental mapping of AZ31/CNT/nHa alloy.

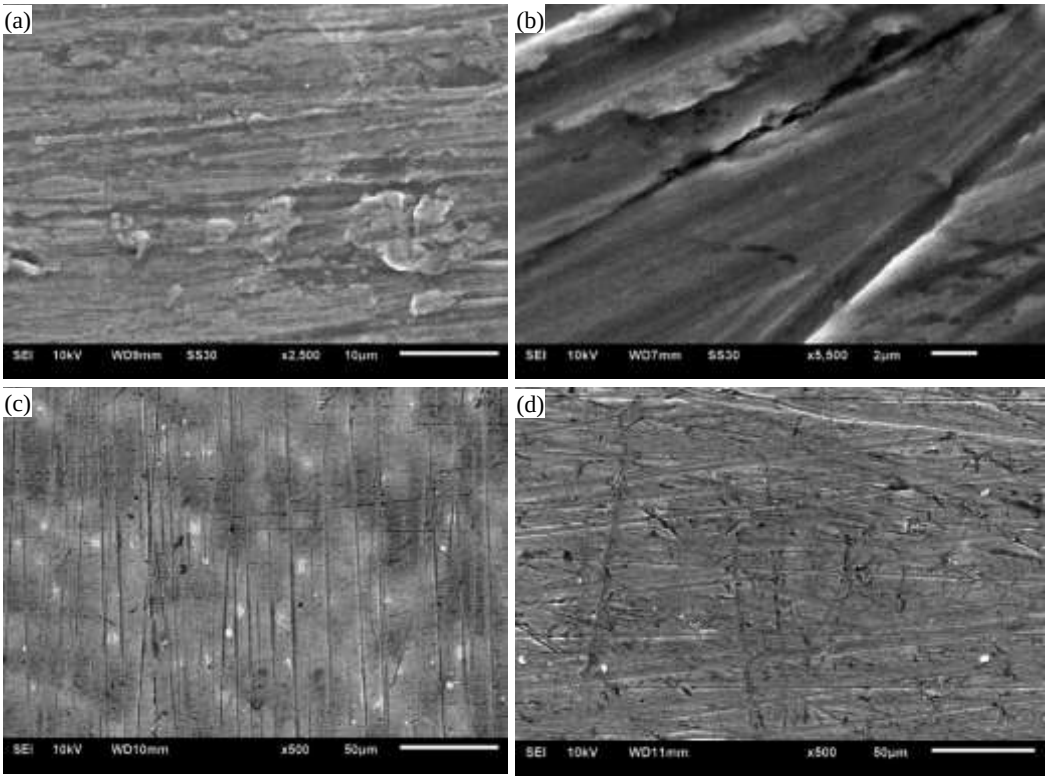

Figure 3. Scanning electron microscopy micrograph representing particle agglomerations, air gap, wear debris, and patches on the surface.

Table 2. Mechanical and physical characteristics of AZ31 alloy and AZ31/CNT/nHA composites.

S. N.	Base material (AZ31) (Weight %)	Reinforcement 1 (CNT) (Weight %)	Reinforcement 2 (nHA) (Weight %)	Porosity (%)	Hardness (HV)	Tensile Strength (MPa)	Compression Strength (MPa)
1	100	0	0	0.43	63	195	90
2	99	0.5	0.5	2.18	84	220	188
3	98.5	1	0.5	2.34	87	234	215
4	97.5	2	0.5	2.48	89	245	228
5	95.5	4	0.5	5.30	77	228	210

Figure 4 shows the tensile yield strength of composites containing varying quantities of CNTs and 0.5% nHA. The inclusion of CNTs/nHA greatly increased the tensile yield strength of the AZ31 alloy, attained a highest value of 245 MPa with 2.0 wt.% CNTs. The tensile strength of the pure AZ31 alloy was measured at 195 MPa. The tensile strength diminshed when the proportion of wt of CNTs approached 4.0 wt.%, which might be due to the development of CNTs clusters in the alloy. As previously documented, these CNT clusters may inhibit efficient interaction among the matrix and CNTs, resulting in microscopic fractures [45], which may elevate permeability in the matrix, resulting in nanocomposite failure with decreased strength [46].

Figure 5 deptics the compressive strength of composites with different quantities of CNTs and 0.5% nHA. The inclusion of CNTs/nHA notably improved the compressive strength of the AZ31 alloy, reaching a peak of 228 MPa with 2.0 wt.% CNTs. The compressive strength of the pure AZ31 matrix was measured as 90 MPa. The compressive strength diminshed when the wt proportion of CNTs surpassed 2.0 wt.%. Previous works have shown that CNTs had a greater influence on compressive characteristics as compared to tensile characteristics, which might be related to considerable strain areas around CNTs caused by entangled shifts in fine-grained CNTs/AZ31 composites undergoing the process of plastic deformation.

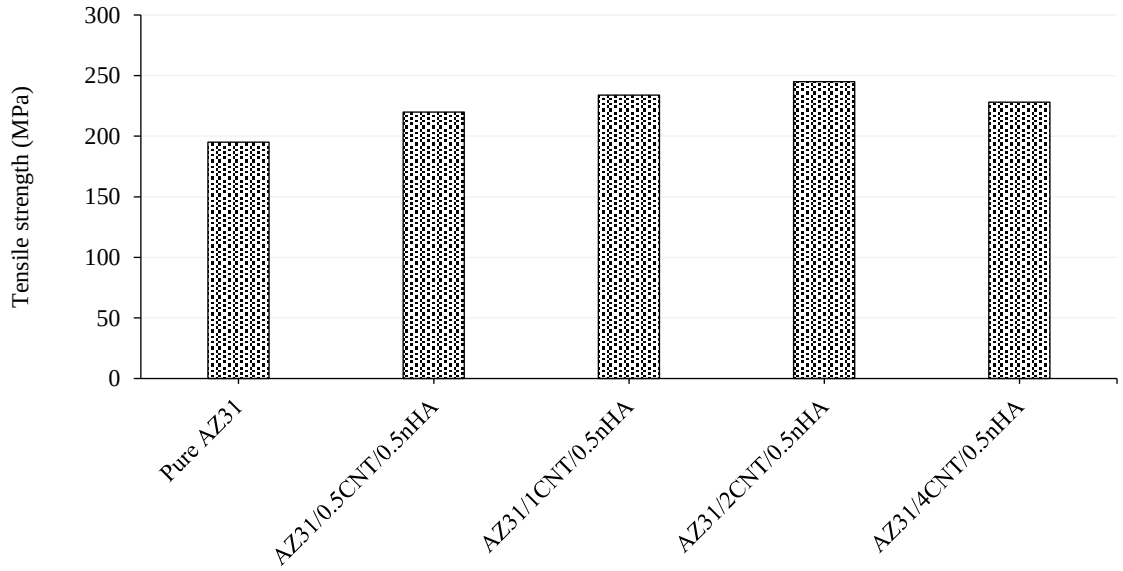

Figure 4. Mean tensile strength of AZ31 alloy and AZ31/CNT/nHA composite.

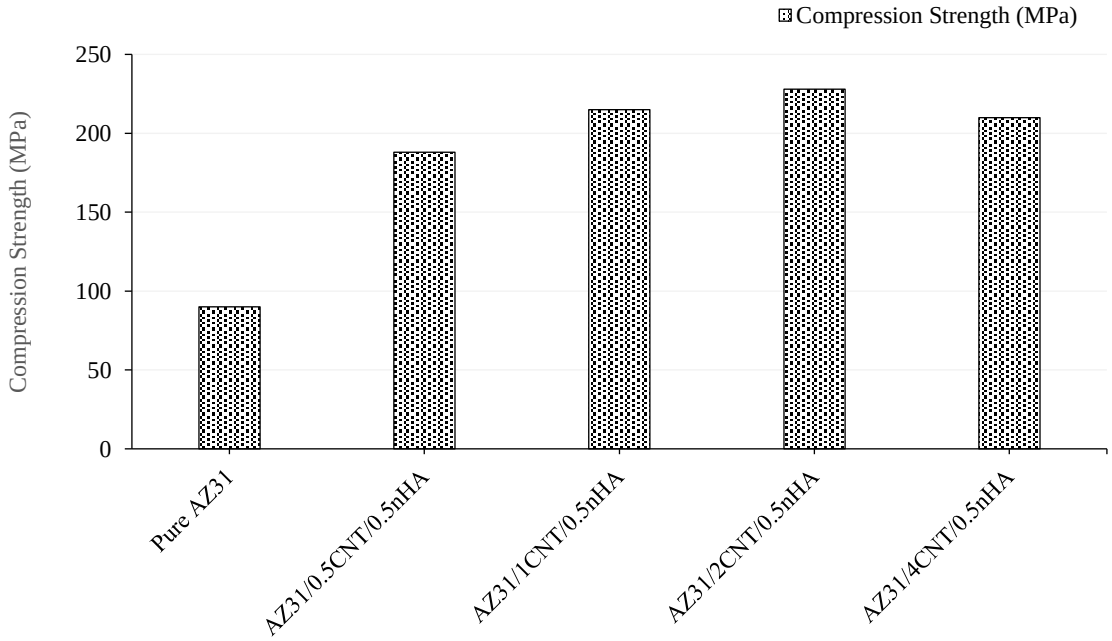

Figure 5. Mean compressive strength of AZ31 alloy and AZ31/CNT/nHA composite.

Figure 6 depicts how CNTs/nHA reinforcements affect nanocomposite hardness. The figure depicts the viker hardness of both the AZ31 matrix and its nanocomposites with varying proportions of reinforcements. As demonstrated in Figure 6, the alloy's microhardness (HV) rose as the proportion of CNTs enhanced, attaining a maximum of HV = 89 for 2.0 wt.% CNT and 0.5% nHA. The hardness of the pure AZ31 matrix was measured as 63. However, microhardness diminished above 2.0 wt.% CNTs. A rise in the hardness may be ascribed to (i) reduction in grain size [47], (ii) CNTs' extreme hardness and tenacity [42], and (iii) the stronger restriction to regional matrix distortion in the time of indentation due to the existence of uniformly distributed CNTs in the alloy [48].

However, the reduction in microhardness can be accounted for by two factors: i) accumulation of CNTs in the composite materials, as shown in Figure 3, and ii) the composites' lower density (higher number of micropores), resulting in reduced microhardness.

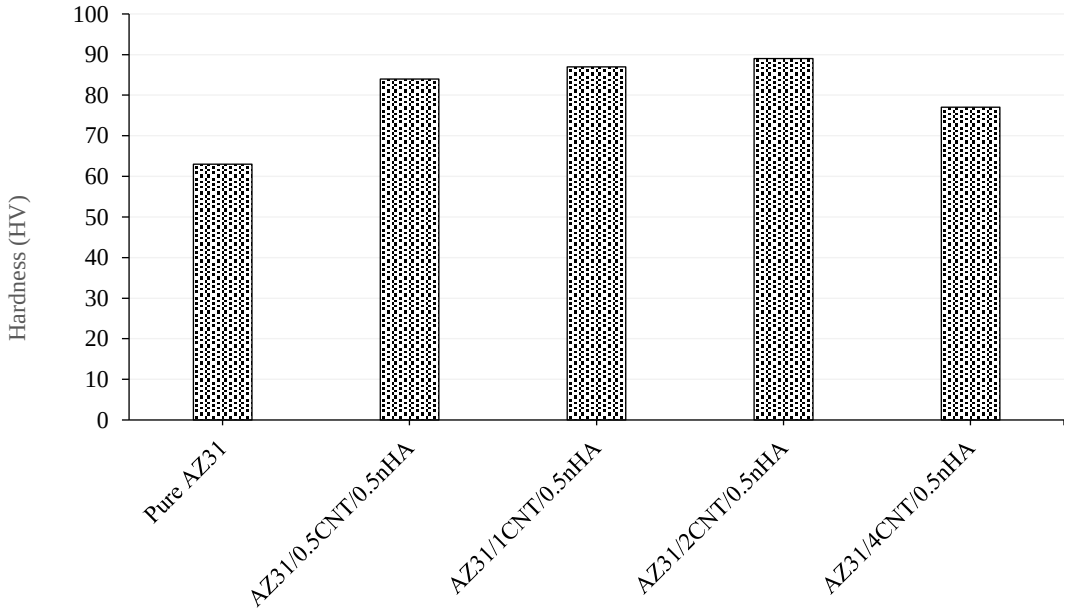

Figure 6. Mean Hardness values of AZ31 alloy and 1/CNT/nHA composite.

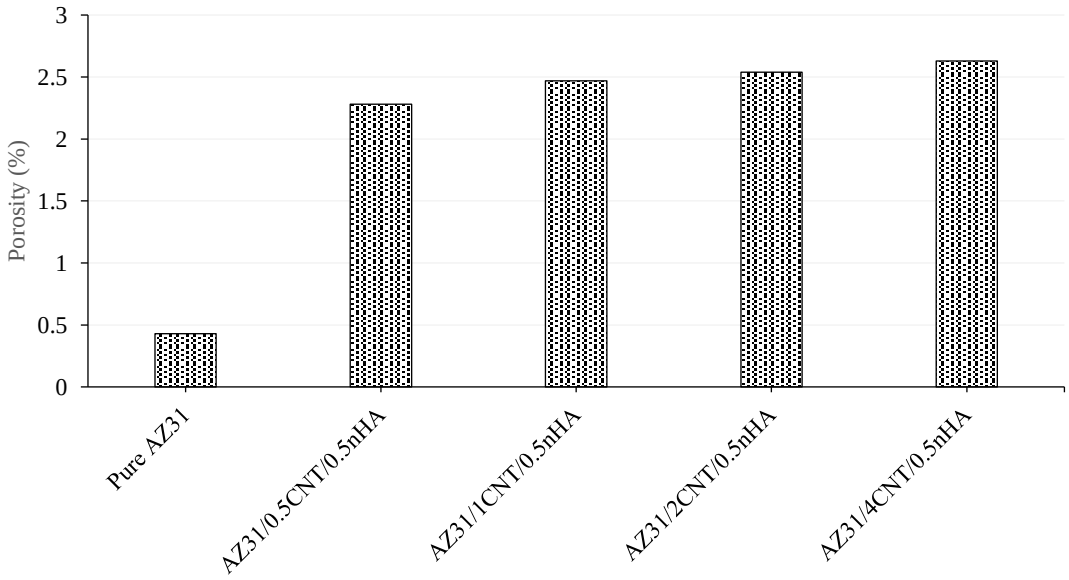

Figure 7. Mean porosity of AZ31 alloy and AZ31/CNT/nHA composite.

The mean porosity of AZ31 alloy and AZ31/CNT/nHA composite is shown in Figure 7. The porosity of AZ31 rises progressively as the weight proportion of CNTs increases, reaching a limit of roughly 2.48 wt%. However, above 2.48 wt% of CNTs, there was a significant decrease in porosity, around 5.3%, resulting in the development of CNT clusters in MMCs. At 4 wt% of CNTs, an aggregation of CNTs forms, resulting in a huge dark region along the grain boundaries, and CNTs agglomerate owing to high porosity. The research revealed that the creation of clusters reduces the link between matrices and CNTs, resulting in fractures with reduced strength.

CONCLUSION

The effect of variation of CNT wt% and reinforcement of nHA (0.5 wt%) on the mechanical, physical, and microstructural characteristics of AZ31 composites was examined, and the following findings are obtained in the present study:

- The EDS analysis reveals the presence of components such as C, Zn, Ca, P, O, Mg, and Al in desired proportions on the sample surface and the low-level oxygen spikes resulting in excellent protection against oxygen from the surrounding. However, friction stir casting is an effective approach for developing reinforced composites with the appropriate component proportions.
- The addition of CNTs/nHA noticeably increased the tensile strength of the AZ31 matrix, reaching its peak at 245 MPa with a 2wt% addition of CNTs. In comparison, the pure AZ31 matrix exhibited a tensile strength of 195 MPa. However, increasing the CNT weight percentage beyond 2wt% resulted in a decline in tensile strength. Specifically, at 4wt% CNTs, the tensile strength measured 228 MPa, marking a 7.46% decrease compared to the strength achieved at 2wt% CNTs.
- The incorporation of CNTs/nHA notably improved the compressive strength of the AZ31 matrix, attained highest value of 228 MPa with the addition of 2.0 wt. % CNTs. This value represented a substantial 153.3% increase compared to the compression strength of the pure AZ31 matrix.
- The hardness of the pure AZ31 matrix was observed value of 63 (HV). The hardness of the AZ31 matrix improved with the enhancing amount of CNTs and attained highest value of 89 (HV) at 2.0 wt. % of CNTs, which was 41.26% higher than pure AZ31 matrix.
- The porosity of the composites exhibited an upward trend corresponding to the rise in CNT content, with measured values of 0.43%, 2.18%, 2.34%, 2.48%, and 5.3% at 0wt%, 0.5wt%, 1wt%, 2wt%, and 4wt%, respectively.

Acknowledgement

The author(s) duly acknowledge DCRUST, Murthal for providing infrastructural facilities.

Declaration of interest

The author(s) declare that they have no known competing financial interests or personal relationships that could have appeared to influence the work reported in this paper.

Data availability statement

All the required data is available in the manuscript

REFERENCE

1. Staiger MP, Pietak AM, Huadmai J, Dias G. Magnesium and its alloys as orthopedic biomaterials: a review. Biomaterials 2006;27:1728–34.
2. Almeshaal, M., Palanisamy, S., Murugesan, T. M., Palaniappan, M., & Santulli, C. (2022). Physico-chemical characterization of Grewia Monticola Sond (GMS) fibers for prospective application in biocomposites. Journal of Natural Fibers, 19(17), 15276–15290. https://doi.org/10.1080/15440478.2022.2123076
3. Witte F. The history of biodegradable magnesium implants: a review. Acta Biomater 2010;6:1680–92.
4. Song G. Control of biodegradation of biocompatable magnesium alloys. Corros Sci 2007;49:1696–701.
5. Palanisamy S, Kalimuthu M, Azeez A, Palaniappan M, Dharmalingam S, Nagarajan R, Santulli C. Wear Properties and Post-Moisture Absorption Mechanical Behavior of Kenaf/Banana-Fiber-Reinforced Epoxy Composites. Fibers. 2022; 10(4):32. https://doi.org/10.3390/fib10040032
6. Witte F, Fischer J, Nellesen J, Crostack H-A, Kaese V, Pisch A, et al. In vitro and in vivo corrosion measurements of magnesium alloys. Biomaterials 2006;27:1013–8.
7. Witte F, Hort N, Vogt C, Cohen S, Kainer KU, Willumeit R, et al. Degradable biomaterials based on magnesium corrosion. Curr Opin Solid State Mater Sci 2008;12:63–72.
8. Wang Y, Wei M, Gao J, Hu J, Zhang Y. Corrosion process of pure magnesium in simulated body fluid. Mater Lett 2008;62:2181–4.
9. McBride ED. Magnesium screw and nail transfixion in fractures. South Med J 1938;31:508–14.

10. Palaniappan, M., Palanisamy, S., Murugesan, T.M. et al. Novel Ficus retusa L. aerial root fiber: a sustainable alternative for synthetic fibres in polymer composites reinforcement. Biomass Conv. Bioref. 15, 7585–7601 (2025). https://doi.org/10.1007/s13399-024-05495-4
11. Keim S, Brunner JG, Fabry B, Virtanen S. Control of magnesium corrosion and biocompatibility with biomimetic coatings. J Biomed Mater Res Part B Appl Biomater 2011;96:84–90.
12. Hornberger H, Virtanen S, Boccaccini AR. Biomedical coatings on magnesium alloys–a review. Acta Biomater 2012;8:2442–55.
13. Wang H, Estrin Y, Zúberová Z. Bio-corrosion of a magnesium alloy with different processing histories. Mater Lett 2008;62:2476–9.
14. Palaniappan, M., Palanisamy, S., Khan, R. et al. Synthesis and suitability characterization of microcrystalline cellulose from Citrus x sinensis sweet orange peel fruit waste-based biomass for polymer composite applications. J Polym Res 31, 105 (2024). https://doi.org/10.1007/s10965-024-03946-0
15. Shadanbaz S, Dias GJ. Calcium phosphate coatings on magnesium alloys for biomedical applications: a review. Acta Biomater 2012;8:20–30.
16. Wang H, Estrin Y, Fu HM, Song GL, Zúberová Z. The effect of pre-processing and grain structure on the bio-corrosion and fatigue resistance of magnesium alloy AZ31. Adv Eng Mater 2007;9:967–72.
17. Hua Y, Zhang Z, Li W. Microstructure and degradation properties of C-containing composite coatings on magnesium alloy wires treated with micro-arc oxidation. Surf Coatings Technol 2016;291:70–8.
18. Palanisamy, S., Kalimuthu, M., Palaniappan, M., Alavudeen, A., Rajini, N., Santulli, C., … Al-Lohedan, H. (2021). Characterization of Acacia caesia Bark Fibers (ACBFs). Journal of Natural Fibers, 19(15), 10241–10252. https://doi.org/10.1080/15440478.2021.1993493
19. Uddin MS, Hall C, Murphy P. Surface treatments for controlling corrosion rate of biodegradable Mg and Mg-based alloy implants. Sci Technol Adv Mater 2015;16:53501.
20. Suchanek W, Yoshimura M. Processing and properties of hydroxyapatite-based biomaterials for use as hard tissue replacement implants. J Mater Res 1998;13:94–117.
21. Gu X, Zhou W, Zheng Y, Dong L, Xi Y, Chai D. Microstructure, mechanical property, bio-corrosion and cytotoxicity evaluations of Mg/HA composites. Mater Sci Eng C 2010;30:827–32.
22. Witte F, Feyerabend F, Maier P, Fischer J, Störmer M, Blawert C, et al. Biodegradable magnesium–hydroxyapatite metal matrix composites. Biomaterials 2007;28:2163–74.
23. Kumar K, Das A, Prasad SB. Effect of multi-pass friction stir processing on mechanical, microstructural, bioactivity, and corrosion properties of novel magnesium-hopeite composite for biomedical applications. Mater Today Commun 2023;35:105584.
24. Kumar K, Das A, Prasad SB. Novel Bioactive Magnesium-Hopeite composite by friction stir processing for orthopedic implant applications. Proc Inst Mech Eng Part H J Eng Med 2023;237:502–16.
25. Yousefpour F, Jamaati R, Aval HJ. Investigation of microstructure, crystallographic texture, and mechanical behavior of magnesium-based nanocomposite fabricated via multi-pass FSP for biomedical applications. J Mech Behav Biomed Mater 2022;125:104894.
26. Vidal C, Alves P, Alves MM, Carmezim MJ, Fernandes MH, Grenho L, et al. Fabrication of a biodegradable and cytocompatible magnesium/nanohydroxyapatite/fluorapatite composite by upward friction stir processing for biomedical applications. J Mech Behav Biomed Mater 2022;129:105137. https://doi.org/10.1016/j.jmbbm.2022.105137.
27. Ghazizadeh E, Jabbari AH, Sedighi M. In vitro corrosion-fatigue behavior of biodegradable Mg/HA composite in simulated body fluid. J Magnes Alloy 2021;9:2169–84. https://doi.org/10.1016/j.jma.2021.03.027.
28. Dubey A, Jaiswal S, Garg A, Jain V, Lahiri D. Synthesis and evaluation of magnesium/co-precipitated hydroxyapatite based composite for biomedical application. J Mech Behav Biomed Mater 2021;118. https://doi.org/10.1016/j.jmbbm.2021.104460.

29. Khalili V, Moslemi S, Ruttert B, Frenzel J, Theisen W, Eggeler G. Surface metal matrix nano-composite of magnesium/hydroxyapatite produced by stir-centrifugal casting. Surf Coatings Technol 2021;406. https://doi.org/10.1016/j.surfcoat.2020.126654.
30. Jaiswal S, Dubey A, Lahiri D. The influence of bioactive hydroxyapatite shape and size on the mechanical and biodegradation behaviour of magnesium based composite. Ceram Int 2020;46:27205–18. https://doi.org/10.1016/j.ceramint.2020.07.202.
31. Jamel MM, Jamel MM, Lopez HF. Designing Advanced Biomedical Biodegradable Mg Alloys: A Review. Metals (Basel) 2022;12. https://doi.org/10.3390/met12010085.
32. Sharma SK, Saxena KK, Kumar KB, Kumar N. The effect of reinforcements on the mechanical properties of AZ31 composites prepared by powder metallurgy: An overview. Mater Today Proc 2022;56:2293–9.
33. Abazari S, Shamsipur A, Bakhsheshi-Rad HR, Keshavarz M, Kehtari M, Ramakrishna S, et al. MgO-incorporated carbon nanotubes-reinforced Mg-based composites to improve mechanical, corrosion, and biological properties targeting biomedical applications. J Mater Res Technol 2022;20:976–90.
34. Zhou M, Qu X, Ren L, Fan L, Zhang Y, Guo Y, et al. The effects of carbon nanotubes on the mechanical and wear properties of AZ31 alloy. Materials (Basel) 2017;10:1385.
35. Mikhalchan A, Vilatela JJ. A perspective on high-performance CNT fibres for structural composites. Carbon N Y 2019;150:191–215.
36. Coleman JN, Khan U, Gun'ko YK. Mechanical reinforcement of polymers using carbon nanotubes. Adv Mater 2006;18:689–706.
37. Bagheri B, Abdollahzadeh A, Sharifi F, Abbasi M. The role of vibration and pass number on microstructure and mechanical properties of AZ91/SiC composite layer during friction stir processing. Proc Inst Mech Eng Part C J Mech Eng Sci 2022;236:2312–26. https://doi.org/10.1177/09544062211024281.
38. Pina S, Oliveira JM, Reis RL. Natural-based nanocomposites for bone tissue engineering and regenerative medicine: A review. Adv Mater 2015;27:1143–69.
39. Singh G, Singh RP, Jolly SS. Customized hydroxyapatites for bone-tissue engineering and drug delivery applications: A review. J Sol-Gel Sci Technol 2020;94:505–30.
40. Zhao X, Chen X, Zhang L, Liu Q, Wang Y, Zhang W, et al. Preparation of nano-hydroxyapatite coated carbon nanotube reinforced hydroxyapatite composites. Coatings 2018;8:357.
41. Mohanasundaram S, Bhong M, Vatsa G, Verma RP, Srivastava M, Kumar G, et al. Mg-based metal matrix composite in biomedical applications: a review. Mater Today Proc 2023.
42. Pietrzykowska E, Romelczyk-Baishya B, Chodara A, Koltsov I, Smogór H, Mizeracki J, et al. Microstructure and mechanical properties of inverse nanocomposite made from polylactide and hydroxyapatite nanoparticles. Materials (Basel) 2021;15:184.
43. Du Z, Tan MJ, Guo JF, Bi G, Wei J. Fabrication of a new Al-Al2O3-CNTs composite using friction stir processing (FSP). Mater Sci Eng A 2016;667:125–31. https://doi.org/10.1016/j.msea.2016.04.094.
44. Li CD, Wang XJ, Liu WQ, Wu K, Shi HL, Ding C, et al. Microstructure and strengthening mechanism of carbon nanotubes reinforced magnesium matrix composite. Mater Sci Eng A 2014;597:264–9. https://doi.org/10.1016/j.msea.2014.01.008.
45. Goh CS, Wei J, Lee LC, Gupta M. Development of novel carbon nanotube reinforced magnesium nanocomposites using the powder metallurgy technique. Nanotechnology 2006;17:7–12. https://doi.org/10.1088/0957-4484/17/1/002.
46. Hassan HA, Lewandowski JJ. Effects of particulate volume fraction on cyclic stress response and fatigue life of AZ91D magnesium alloy metal matrix composites. Mater Sci Eng A 2014;600:188–94. https://doi.org/10.1016/j.msea.2014.02.021.
47. Rashad M, Pan F, Zhang J, Asif M. Use of high energy ball milling to study the role of graphene nanoplatelets and carbon nanotubes reinforced magnesium alloy. J Alloys Compd 2015;646:223–32. https://doi.org/10.1016/j.jallcom.2015.06.051.

48. Kumar Sharma S, Kumar Saxena K. Effects on microstructure and mechanical properties of AZ31 reinforced with CNT by powder metallurgy: An overview. Mater Today Proc 2022;56:2038–42. https://doi.org/10.1016/j.matpr.2021.11.376.

